

Closed-Form Equation for Thermal Constriction/Spreading Resistances with Variable Resistance Boundary Condition

By

Seaho Song¹, Seri Lee², and Van Au¹

¹Bell-Northern Research Ltd, Ottawa, Ontario, Canada

²Aavid Engineering, Inc., Laconia, NH

ABSTRACT

Simple equations are developed for predicting thermal constriction/spreading resistances associated with heat transfer in electronics packaging applications.

KEYWORDS

constriction resistance, spreading resistance

INTRODUCTION

Whenever heat flows through one or more solids involving a change in cross-sectional area, there is a resistance associated with the spreading or constricting of heat flow. Rarely in electronics packaging applications does a heat transfer analysis exclude estimates of constriction/spreading resistances. Figure 1 shows a typical example where constriction and spreading resistances occur within the path of heat flow. There is no simple expression presently available to predict these resistances.

There exist special case solutions by Yovanovich [Aung, 1991] and Mikic [Kraus & Bar-Cohen, 1983] where the heat spreader base is assumed to be either infinitely wide and/or infinitely thick. These solutions, because of the idealized boundary condition assumptions, are seldom of use in electronics packaging thermal problems. For a plate with finite dimensions, Kennedy [1960] developed a series solution for a special case where the bottom of the spreader plate is assumed to be at a constant temperature, and this solution has been widely used in the packaging industry for some thirty-five years. However, the constant temperature assumption (at the bottom of the plate) results in an optimistic solution which may be inaccurate by an order of magnitude.

In the present paper, equations for thermal constriction/spreading resistances are developed for cases where the boundary condition for the spreader plate is non-isothermal. The equations are approximate in nature, but they are explicit and simple to use. The accuracy of the equations are verified through available numerical data.

CONSTRICION/SPREADING RESISTANCE

The present work considers a disc-shaped spreader plate (Figure 2) with radius b and thickness t , and a uniform circular heat source on the top with radius a . *The* plate is assumed to be insulated everywhere except the heat source area and the bottom, where a uniform heat transfer coefficient boundary condition exists (here expressed in terms of an external resistance R_o). *The* use of an external resistance R_o allows a realistic boundary condition (over the isothermal case). Note that as the external resistance approaches zero, the boundary condition approaches the isothermal case.

Recent numerical work by Naraghi and Antonetti [1993] allows the spreading resistance solutions for the circular geometry applicable to other geometries (Figure 3). Equivalent source and base radii are defined as:

$$a = \sqrt{\frac{A_s}{\pi}} \quad (1)$$

$$b = \sqrt{\frac{A_b}{\pi}} \quad (2)$$

where A_s and A_b are the heat source and the spreader base areas, respectively.

An average thermal spreading resistance is defined as:

$$R_{avg} = \frac{\overline{T}_s - \overline{T}_b}{Q} \quad (3)$$

where \overline{T}_s and \overline{T}_b are average temperatures over the source and base areas, respectively, and Q is the total heat transfer rate. It should be noted that R_{avg} defined in Equation 3 actually includes both the spreading resistance and the bulk material resistance associated with the plate thickness t .

Similarly a maximum thermal spreading resistance is defined as:

$$R_{max} = \frac{T_{max} - \bar{T}_b}{Q} \quad (4)$$

where T_{max} is the maximum temperature in the heat source area. This resistance notation is useful when the temperature gradient within the heat source area is of interest.

Thermal spreading resistance solutions require five input parameters, a , b , t , k , and R_o :

$$R_{avg} = fn(a, b, t, k, R_o) \quad (5)$$

$$R_{max} = fn(a, b, t, k, R_o) \quad (6)$$

To simplify the presentation of solutions, the following dimensionless parameters are introduced:

$$\text{dimensionless heat source radius} \quad \epsilon = \frac{a}{b} \quad (7)$$

$$\text{dimensionless plate thickness} \quad \tau = \frac{t}{b} \quad (8)$$

$$\text{effective Biot Number} \quad Bi = \frac{1}{R_o \cdot (\pi \cdot b^2)} \cdot \frac{b}{k} = \frac{1}{\pi \cdot k \cdot b \cdot R_o} \quad (9)$$

$$\text{dimensionless resistance} \quad \Psi = \sqrt{\pi} \cdot k \cdot a \cdot R \quad (10)$$

With the above normalization the solutions for spreading resistances can be presented in terms of only three parameters, ϵ , τ , and Bi :

$$\Psi_{avg} = \sqrt{\pi} \cdot k \cdot a \cdot R_{avg} = fn(\epsilon, \tau, Bi) \quad (11)$$

$$\Psi_{max} = \sqrt{\pi} \cdot k \cdot a \cdot R_{max} = fn(\epsilon, \tau, Bi) \quad (12)$$

It is emphasized again that the resistance notations in Equations 11 & 12 include the bulk material resistance, normally estimated as $\frac{t}{k \cdot A_b}$.

CLOSED-FORM EQUATION

Analytical solutions for spreading resistance for the configuration shown in Figure 2 has recently been developed by the present authors, and have been submitted for publication elsewhere (Lee et. al [1995]). These solutions are in the form of an infinite series with special functions, and require computation of a few hundred terms.

Using the analytical solutions, the present authors have developed approximate congelations, and they are presented here:

$$\Psi_{avg} = \frac{\varepsilon \cdot \tau}{\sqrt{\pi}} + \frac{1}{2} \cdot (1 - \varepsilon)^2 \cdot \Phi_c \quad (13)$$

$$\Psi_{max} = \frac{\varepsilon \cdot \tau}{\sqrt{\pi}} + \frac{1}{\sqrt{\pi}} \cdot (1 - \varepsilon) \cdot \Phi_c \quad (14)$$

where

$$\Phi_c = \frac{\tanh(\lambda_c \cdot \tau) + \frac{\lambda_c}{Bi}}{1 + \frac{\lambda_c}{Bi} \cdot \tanh(\lambda_c \cdot \tau)} \quad (15)$$

with

$$\lambda_c = \pi + \frac{1}{\sqrt{\pi \cdot \varepsilon}} \quad (16)$$

These approximate equations are explicit and simple to use. The predictions from these equations of maximum dimensionless resistances are compared with numerical solutions by Nelson and Sayers [1992] in Figure 4. The comparison shows excellent agreement, in general well within 10 percent.

APPLICATION EXAMPLE WITH EXPERIMENTAL VERIFICATION

In this section, an example analysis is provided to demonstrate the use of Equations 13 thru 16. Experiments were performed to verify analysis results, and these are also discussed in this section. Figure 5 shows an example where a heat source is attached to an oversized heat sink. Consider a heat sink with base dimensions, 100mm x 100mm x 3mm, and fourteen fins (25mm high x 100mm long x

2mm thick). One wishes to determine the thermal resistance associated **with** the heat path from the heat source through the heat sink to the ambient (air). The lumped heat sink resistance, R_{hs} , consists of two resistances $R_{fin-air}$ and R_{spread} , which are the heat sink to ambient and spreading resistances, respectively, and are defined as:

$$R_{fin-air} = \frac{1}{h \cdot \eta \cdot A_{fin}} \quad (17)$$

$$R_{spread} = \frac{\Psi}{\sqrt{\pi k_{hs} a_s}} \quad (18)$$

The spreading resistance, R_{spread} , from the heat source through the heat sink base is estimated using Ψ correlations presented in Equations 13 thru 16. The thermal resistance between the fins and ambient, $R_{fin-air}$, is normally estimated by using correlations for channel flow, or by employing heat sink performance data from a manufacturer. Instead, in the present work $R_{fin-air}$ was measured by attaching a 100mm x 100mm Minco heater (equal in size to the heat sink base area) to the base of the heat sink using Chomerics T404 double-sided thermal tape. With its base insulated, the heat sink was placed inside a wind tunnel and was exposed to air velocities of 1, 3, and 5 m/s. The base and ambient temperatures were measured using thermocouples epoxied inside 0.75mm wide x 1.0mm deep grooves that were milled into the base of the heat sink. The external resistance, $R_{fin-air}$, was determined as

$$R_{fin-air} = \frac{\bar{T}_b - T_{amb}}{q} \quad (19)$$

where \bar{T}_b is the average temperature at the heat sink base. The external resistance measurements for three air velocities yielded effective Biot numbers of 0.046, 0.074, and 0.099.

Additional experiments were performed, using the above heat sink under similar flow conditions, for two heat source sizes: 25.4mm x 25.4mm and 8.9mm x 10.2mm ($a = 14.3mm$ and $5.4mm$), respectively. The experimental $R_{hs avg}$ and $R_{hs max}$ were determined by

$$R_{hs avg} = \frac{\bar{T}_s - T_{amb}}{Q} \quad (20)$$

$$R_{hs max} = \frac{T_{max} - T_{amb}}{Q} \quad (21)$$

Dimensionless spreading resistances Ψ_{avg} and Ψ_{max} were calculated for two heat source sizes ($a = 14.3mm$ and $5.4mm$) for Biot numbers of 0.046, 0.074, and 0.099. These were then converted to dimensional resistances using Equation 18. The average and maximum heat sink resistances were computed as the sum of the two distinct resistances:

$$R_{hs\ avg} = R_{fin-air} + R_{spread\ avg} \quad (22)$$

$$R_{hs\ max} = R_{fin-air} + R_{spread\ max} \quad (23)$$

Both calculated and experimental results for average and maximum heat sink resistances under forced convection with variable heat source sizes are summarized in Tables 1 and 2, respectively. Calculated and experimental results agree in general within 10%.

					Measured	Calculated			Measured	
a [m]	Velocity [m/s]	ϵ	τ	Bi	$R_{fin-air}$ [°C/W]	Ψ_{avg}	$R_{spread\ avg}$ [°C/W]	$R_{hs\ avg}$ [°C/W]	$R_{hs\ avg}$ [°C/W]	% Difference
0.014	1	0.247	0.086	0.046	0.79	0.750	0.20	0.98	1.07	-9.2
	3			0.074	0.49	0.743	0.20	0.69	0.75	-8.7
	5			0.099	0.37	0.737	0.19	0.56	0.63	-12.5
0.0054	1	0.092	0.086	0.046	0.79	0.655	0.46	1.25	N/A	N/A
	3			0.074	0.49	0.653	0.46	0.95	N/A	N/A
	5			0.099	0.37	0.652	0.46	0.82	N/A	N/A

Table 1: Comparison of calculated and measured average heat sink resistance, $R_{hs\ avg}$, with variable convection conditions and heat source sizes ($b = 58\ mm$, $t = 3\ mm$).

					Measured	Calculated			Measured	
[m]	Velocity [n-h]	ϵ	τ	Bi	$R_{fin-air}$ [°C/W]	Ψ_{max}	$R_{spread\ max}$ [°C/W]	$R_{hs\ max}$ [°C/W]	$R_{hs\ max}$ [°C/W]	% Difference
0.014	1	0.247	0.086	0.046	0.79	0.971	0.25	1.04	1.12	-7.7
	3			0.074	0.49	0.962	0.25	0.74	0.80	-8.1
	5			0.099	0.37	0.955	0.25	0.62	0.68	-9.7
0.0054	1	0.092	0.086	0.046	0.79	0.774	0.54	1.33	1.35	-1.5
	3			0.074	0.49	0.773	0.54	1.03	1.04	-1.0
	5			0.099	0.37	0.771	0.54	0.91	0.91	0

Table 2: Comparison of calculated and measured maximum heat sink resistance, $R_{hs\ max}$, with variable convection conditions and heat source sizes ($b = 58\ mm$, $t = 3\ mm$).

Charts for average and maximum constriction/spreading resistances are shown in Figures 6 & 7. These charts were produced using the exact solutions developed by the present authors (Lee et. al [1995]). These charts are included in this paper to provide a thermal designer with alternate means (to Equations 13- 16) of estimating constriction/spreading resistances.

SUMMARY

Closed form correlation equations were developed to predict average and maximum thermal constriction/spreading resistances. The accuracy of the equations was verified using available numerical solutions. A thermal analysis example was presented to demonstrate the usefulness of the equations.

REFERENCES

Aung, W., 1991, *Cooling Techniques for Computers*, Hemisphere Pub. Corp., New York

Kennedy, D.P., 1960, "Spreading Resistance in Cylindrical Semiconductor Devices", *Journal of Applied Physics*, Vol. 31, pp. 1490-1497.

Kraus, D.A., and Bar-Cohen, A., 1983, *Thermal Analysis and Control of Electronic Equipment*, McGraw Hill.

Naraghi, M.H.N., and Antonetti, V.W., 1993, "Macro-Constriction Resistance of Distributed Contact Contour Areas in a Vacuum Environment", Paper presented at the ASME Winter Annual Meeting, New Orleans, La, Nov. 28- Dec. 3.

Lee, S., Song, S., Au, V., and Moran, K.P., 1995, "Constriction/Spreading Resistance Model for Electronics Packaging", Paper submitted for presentation at the 4th ASME/JSME Thermal Engineering Joint Conference, March 19-24, Maui, Hawaii.

Nelson, D.J., and Sayers, W.A., 1992, "A Comparison of Two-Dimensional Planar, Axisymmetric and Three-Dimensional Spreading Resistances", *Proceedings of 8th Annual IEEE Semiconductor Thermal Measurement and Management Symposium*, Austin, TX, Feb. 3-5.

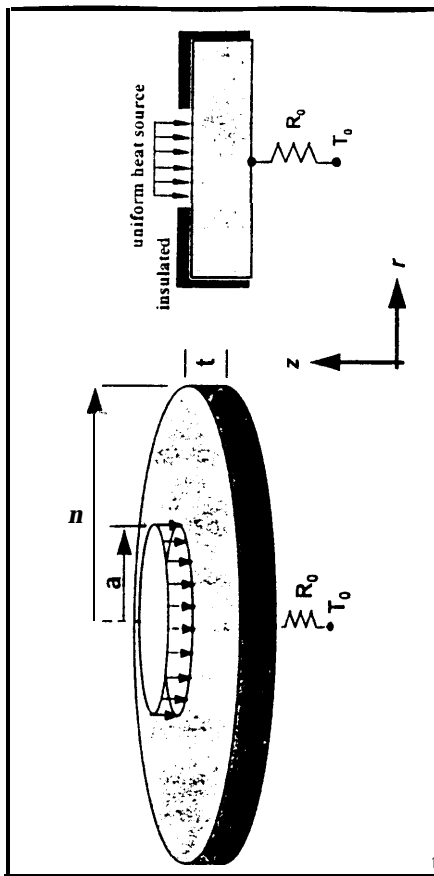


FIGURE 2: Constriction/Spreading Resistance Model

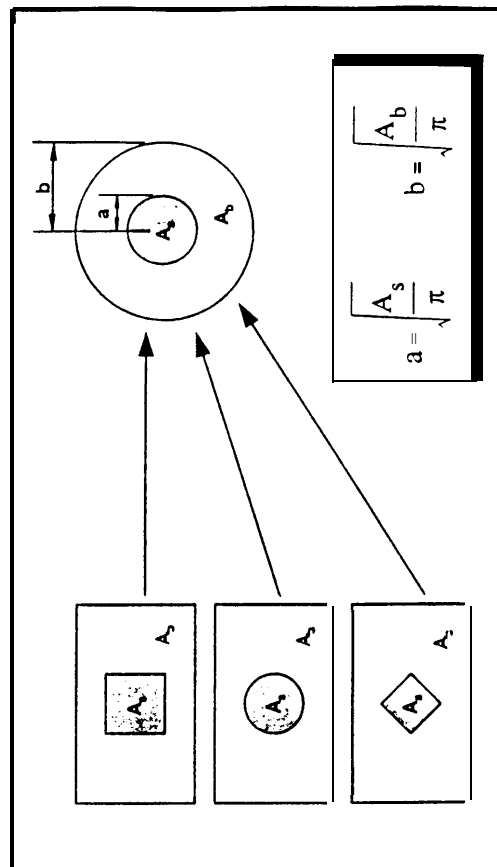


FIGURE 3: Area Shape Conversion for Effective Radii. a and b

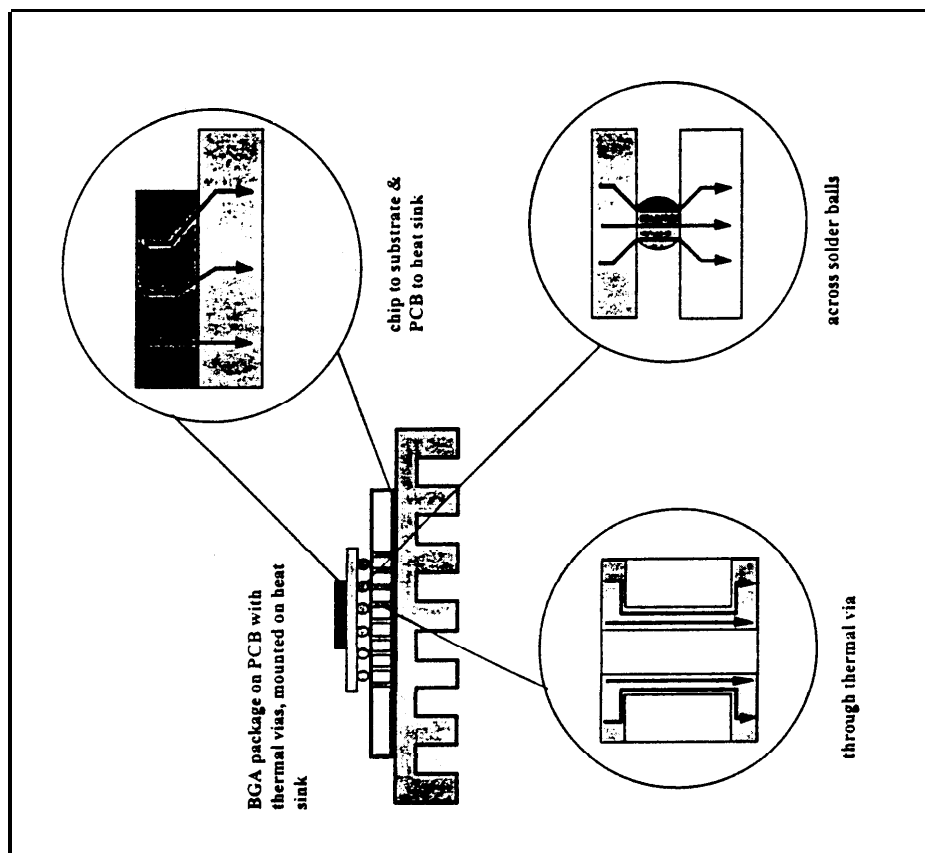


FIGURE 1: Thermal Constriction/Spreading Resistances in Electronics Packaging

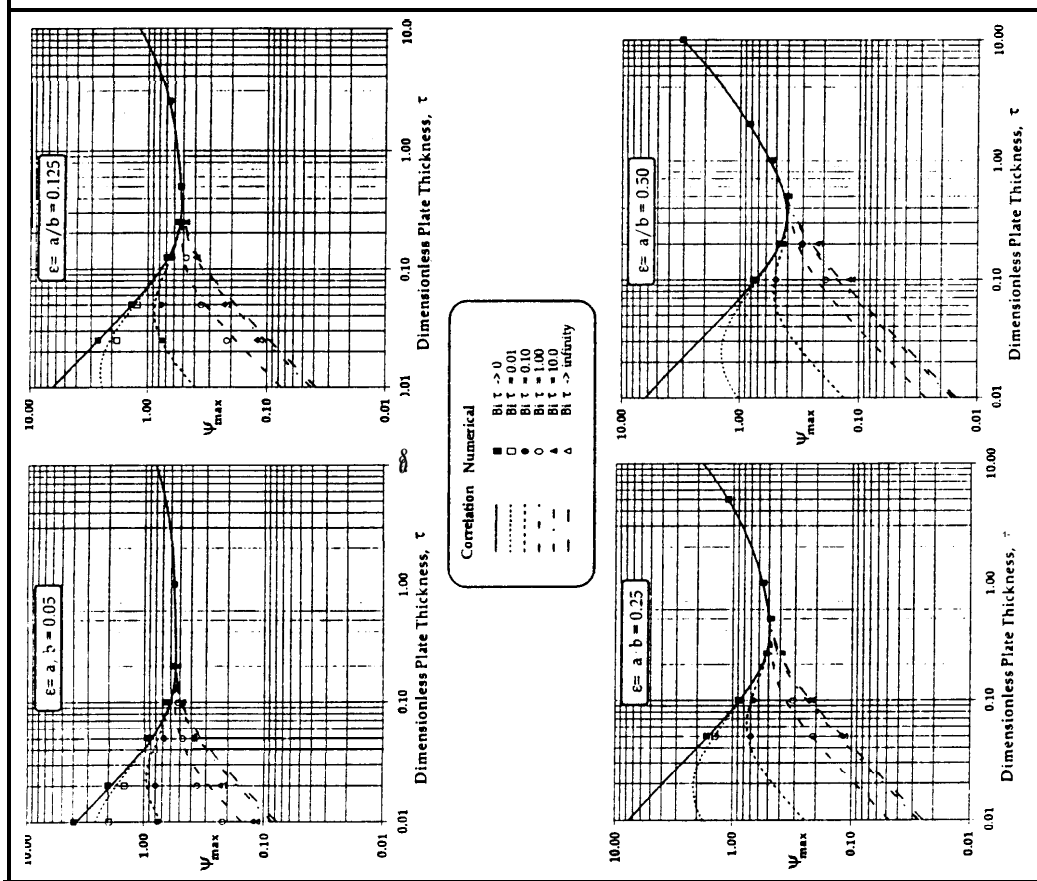


FIGURE 4 : Comparison of Correlation with Nelson & Sayers [1992]

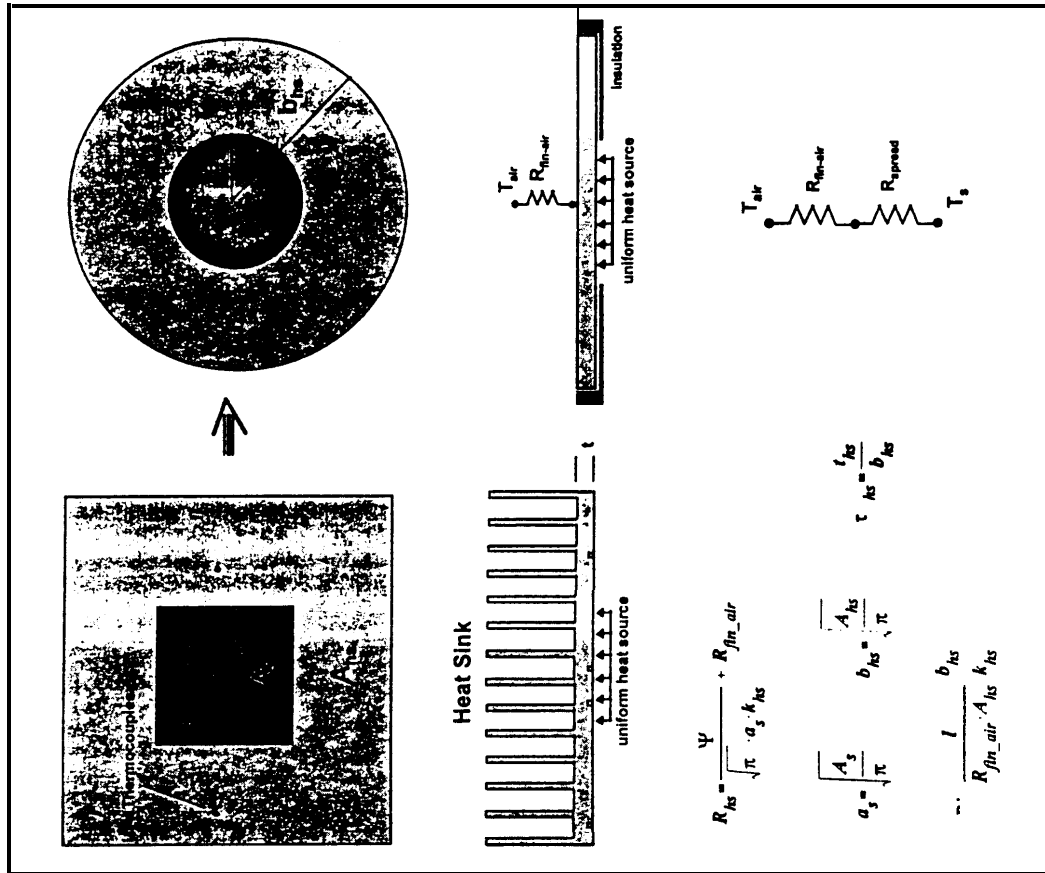


FIGURE 5: Modeling example Using Correlation

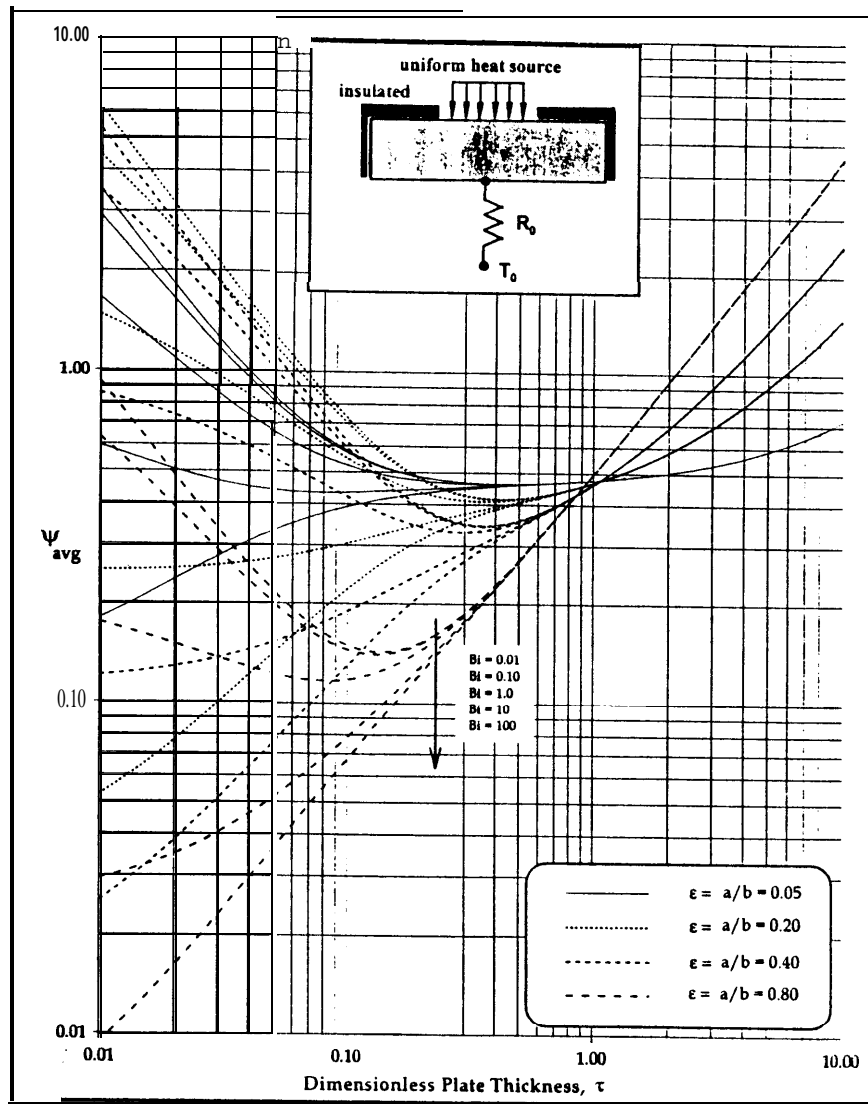


FIGURE 6: Average Constriction/Spreading Resistance Chart

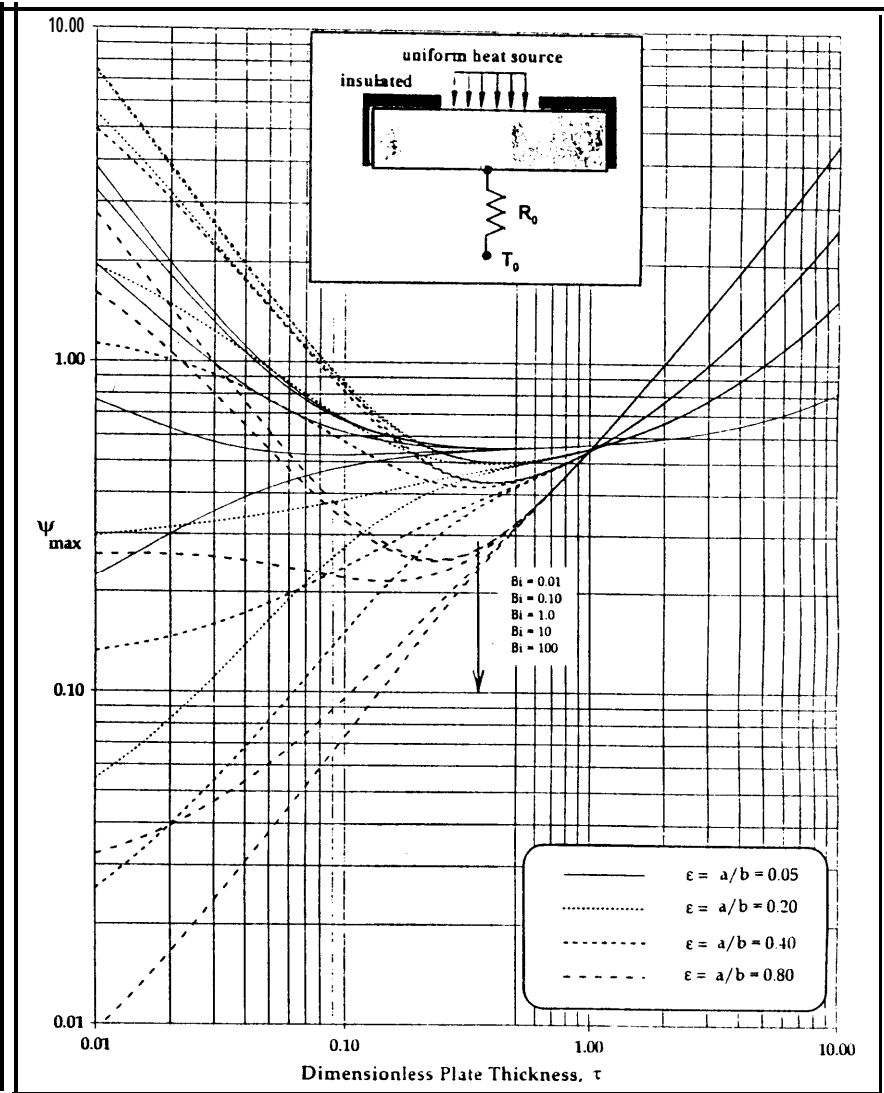


FIGURE 7: Maximum Constriction/Spreading Resistance Chart